Mechanisms of Ranolazine Pretreatment in Preventing Ventricular Tachyarrhythmias in Diabetic db/db Mice with Acute Regional Ischemia-Reperfusion Injury

Chung-Chuan Chou
Chang Gung Memorial Hospital https://orcid.org/0000-0003-4465-0016
Hui-Ling Lee
Chang Gung Memorial Hospital
Gwo-Jyh Chang
Chang Gung University School of Medicine
Hung-Ta Wo
Chiayi Chang Gung Memorial Hospital
Tzung-Hai Yen
Chang Gung Memorial Hospital
Ming-Shien Wen
Chang Gung Memorial Hospital
Yen Chu
Chang Gung Memorial Hospital
Hao-Tien Liu
Chang Gung Memorial Hospital
Po-Cheng Chang (pccbrian@gmail.com)
https://orcid.org/0000-0002-6901-5951

Original investigation

Keywords: late sodium current; myocardial ischemia-reperfusion; db/db mouse; optical mapping; ventricular tachyarrhythmia

Posted Date: March 16th, 2020

DOI: https://doi.org/10.21203/rs.3.rs-17242/v1

Abstract

Background: Studies have demonstrated that db/db mice have increased susceptibility to myocardial ischemia-reperfusion (IR) injury and ventricular tachyarrhythmias (VA). We aimed to investigate the antiarrhythmic and molecular mechanisms of ranolazine in db/db mouse hearts with acute IR injury.

Methods: Ranolazine was administered for 1 week before coronary artery ligation. Diabetic db/db and control db/+ mice were divided into ranolazine-given and -nongiven groups. IR model was created by 15-min left coronary artery ligation and 10-min reperfusion. In vivo electrophysiological studies and optical mapping to simultaneously record intracellular Ca2+ (Cai) and membrane voltage in Langendorff-perfused hearts were performed. Western blotting and whole-cell patch clamp study were performed to evaluate the effect of ranolazine in the non-IR and IR zones.

Results: The severity of VA inducibility by burst pacing was higher in db/db mice than db/+ mice with acute IR injury. Ranolazine suppressed VA inducibility and severity in db/db and db/+ mice. Optical mapping studies showed that ranolazine significantly shortened action potential duration (APD80), Cai transient duration (CaiTD80), Cai decay time, ameliorated conduction inhomogeneity, and suppressed arrhythmogenic alternans induction. The expression of pThr17-phospholamban, calsequestrin 2 and SCN5A in the IR zone was significantly downregulated in db/db mice, which was ameliorated by ranolazine.

Conclusions: Ranolazine pretreatment shortens APD80 and CaiTD80, reduces Cai decay time, and ameliorates conduction velocity inhomogeneity to suppress induction of arrhythmogenic alternans and VA; and amelioration of downregulation of pThr17-phospholamban, calsequestrin 2 and SCN5A may partly underlie the anti-arrhythmic molecular mechanisms of ranolazine in db/db mouse hearts with IR injury.

Background

Studies have demonstrated that diabetic (db/db) mice have increased susceptibility to myocardial ischemia-reperfusion (IR) injury,[1, 2] a longer duration of IR-induced ventricular tachycardia (VT) and more degeneration of VT into ventricular fibrillation (VF),[3] and a greater mortality after IR compared with control (db/+) mice.[4] However, the underlying electrophysiological and molecular mechanisms remain incompletely understood. Accumulation of intracellular Na^+ occurs during IR,[5] and increased late sodium current ($I_{Na,L}$) has been linked to elevated intracellular Na^+ during IR. Upon reperfusion of ischemic myocardium, the sudden availability of oxygen in the ischemic myocardium increases the formation of reactive oxygen species which are known to increase $I_{Na,L}$,[6] thereby worsening intracellular Na^+ overload.[7] Subsequently, intracellular Ca^{2+} (Ca_i) overload occurs via reverse-mode Na^+/Ca^{2+} exchanger (NCX), leading to cell damage, apoptosis, and lethal cardiac arrhythmias. In diabetic mice, it has been reported that phosphoinositide 3-kinase signaling is reduced, resulting in a higher $I_{Na,L}$ in cardiomyocytes from db/db mice than in wild-type cardiomyocytes.[8] A higher intrinsic $I_{Na,L}$ density would play a role in the increased susceptibility to IR arrhythmias in db/db mice. Ranolazine, a clinically used nonspecific blocker of $I_{Na,L}$,[9] was reported to reduce Ca^{2+} overload and oxidative stress, to improve mitochondrial integrity,[10] and to reduce ventricular tachyarrhythmia (VA) induced by IR injury.[11] In this study, we conducted simultaneous Ca_i and membrane voltage (V_m) optical mapping to investigate the arrhythmogenicity of db/db mice with acute IR injury and the antiarrhythmic mechanisms of ranolazine in these hearts. The second aim of the study was to perform Western blotting to investigate the molecular mechanisms underlying ranolazine-induced electrophysiological remodeling.

Methods

This study protocol was approved by the Institutional Animal Care and Use Committee of Chang Gung Memorial Hospital (approval no. 2015092401) and conformed to the current NIH guidelines for the care and use of laboratory animals. The mice were divided into four groups: diabetic mice not given ranolazine (db/db C, n = 22), diabetic mice given ranolazine (db/db R, n = 21), control mice not given ranolazine (db/+ C, n = 23), and control mice given ranolazine (db/+ R, n = 21). Ranolazine (R6152; Sigma-Aldrich, Munich, Germany) was administered orally at 305 mg/kg/d (dose comparable with that used clinically in humans of 750 mg twice daily) for 7 days.

In-vivo IR model creation and electrophysiological studies

Mice were anesthetized with intra-peritoneal injection of xylazine (10 mg/kg) and zoletil (20 mg/kg). After mice appeared fully unconscious, endotracheal intubation was performed for gas general anesthesia with isoflurane (1%). Regional myocardial ischemia was induced by left coronary artery ligation for 15 min, and then the ligature was removed to create the IR model. More detailed descriptions are included in the online supplement.

In vivo electrophysiological study was performed after reperfusion for 10 min.[12] Burst pacing (pacing cycle length (PCL) = 50 ms, 2 sec) and extrastimulus pacing (S_1-S_4) were applied to test VT (≥ three consecutive premature ventricular beats) inducibility to all mice. The severity of

inducible VT was classified as < 10 beats, between 10 to 30 sec, and > 30 beats.[13]

Western Blotting

Cardiac tissues were sampled from the non-IR and IR zones of the left ventricle at the end of in vivo electrophysiological studies for protein quantification as previously described (n = 6 per group).[14] See the online supplement for detailed descriptions.

Langendorff Heart Preparation And Optical Mapping Studies

Details of the experimental procedure for dual optical mapping of V_m and Ca_i transients have been described previously.[15] Briefly, the hearts were excised after reperfusion for 10 min and then subjected to Langendorff-perfusion with Rhod-2AM (Ca_i indicator), RH237 (V_m indicator) and 15 μM blebbistatin (Tocris Bioscience, MN, USA). Epifluorescence was acquired simultaneously using two high-speed cameras (MiCAM Ultima; BrainVision, Tokyo, Japan) at 1 ms/frame. Electrophysiological studies were performed as described in the online supplement.

Cardiomyocyte Isolation And Whole-cell Patch Clamp

Cardiomyocytes from the non-IR and IR zones of the left ventricle were isolated using a modified enzymatic digestion protocol (n = 4 per group).[14] Whole-cell mode of the patch-clamp technique was used to measure I_{Na} as described previously.[16] See the online supplement for detailed descriptions.

Data analysis

Action potential duration at 80% repolarization (APD_{80}) and Ca_i transient duration at 80% decay (Ca_iTD_{80}) were measured at two PCLs of 200 and 100 ms.[12] The differences between the longest and shortest APD_{80} and Ca_iTD_{80} were used to represent APD_{80} and Ca_iTD_{80} dispersion. To estimate conduction velocity (CV), we measured the distance and conduction time between the earliest activation point and two epicardial points: one was from the pacing site to the left ventricular apex (CV_{IR}), and the other was along an axis parallel to the atrioventricular ring (CV_{non-IR}).[17]

Statistics

Continuous variables are expressed as mean ± standard deviation and categorical variables are represented by numbers and percentages. One-way repeated measures analysis of variance with post hoc least significant difference analysis was performed to calculate statistical significance of differences in continuous variables among four groups. Student's t-test was performed to compare continuous variables between the non-IR and IR zones. Categorical variables were tested using Fisher's exact test and post hoc Bonferroni analysis. Differences were considered significant at $P < 0.05$.

Results

Ranolazine suppressed in vivo VA inducibility and severity in mouse hearts with regional IR injury

In the in vivo electrophysiological studies, we acquired data from 7, 7, 8, and 7 mice in the db/db C, db/db R, db/+ C, and db/+ R groups, respectively. The effective refractory period was significantly longer in the db/db C mice than in the db/db R, db/+ C, and db/+ R groups (74 ± 17 vs. 62 ± 18, 58 ± 18, and 60 ± 11 ms, respectively; P = 0.034). Figure 1 summarizes the result of VT inducibility and severity. VT was inducible in 7 of 7, 5 of 7, 8 of 8 and 5 of 7 mice in the db/db C, db/db R, db/+ C, and db/+ R groups, respectively (P = NS, Fig. 1A). But the percentage of VT-induced episodes was higher in the db/db C group compared to the db/+ C group by burst pacing protocol (P = 0.003). Pretreatment of ranolazine significantly reduced the percentage of VT episodes by both burst pacing and extrastimulus pacing protocols in both db/db and db/+ groups (Fig. 1B). Figure 1C shows the number and percentage of VT episodes < 10 beats, between 10 to 30 sec, and > 30 beats in each group. Even if the distribution of VT duration shows most of the VT lasted less than 10 beats, db/db C mice were significantly more vulnerable to longer VTs: Longer VT (> 30 beats) was induced in 5 of 7 (db/db C, the longest 180 beats), 1 of 7 (db/db R, the longest 50 beats), 1 of 8 (db/+ C, the longest 72 beats) and 1 of 7 (db/+ R, the longest 66 beats) hearts (P = 0.031).. A representative example of pacing-induced VT in a db/db C mouse heart is shown in Fig. 1D.

Optical Mapping Studies

Ranolazine effects on APD_{80} and Ca_iTD_{80}

In the optical mapping studies, we acquired data from 11, 10, 11, and 10 mice in the db/db C, db/db R, db/+ C, and db/+ R groups, respectively. As shown in Fig. 2A, the db/db C group tended to have a longer APD_{80} than the db/+ C group. APD_{80} in the db/db C group was significantly longer than that in the db/db R group, but there was no significant difference between the db/+ C and db/+ R groups. In addition, APD_{80} in the IR zone was significantly longer than that in the non-IR zone in the ranolazine non-given groups, but not in the ranolazine given groups (Table 1). The APD_{80} dispersion was significantly different among the 4 groups and the db/db C group had the largest APD_{80} dispersion: at PCL = 200 ms: 27 ± 8, 22 ± 7, 17 ± 5, 16 ± 3 ms in db/db C, db/+ C, db/db R, db/+ R groups, respectively (P = 0.002); at PCL = 100 ms: 17 ± 5, 17 ± 3, 13 ± 3, 13 ± 4 ms in db/db C, db/+ C, db/db R, db/+ R groups, respectively (P = 0.041). Similarly, Ca_iTD_{80} in the db/db C group was significantly longer than that in the db/db R group, and Ca_iTD_{80} in the IR zone was significantly longer than that in the non-IR zone in the ranolazine non-given groups, but not in the ranolazine given groups. The difference of Ca_iTD_{80} dispersion was insignificant at PCL = 200 ms: 23 ± 7, 19 ± 7, 17 ± 8, and 16 ± 6 ms (P = 0.217); but was significant at PCL = 100 ms: 18 ± 7, 18 ± 7, 10 ± 5, and 11 ± 5 ms (P = 0.028) in the db/db C, db/+ C, db/db R, and db/+ R groups, respectively. These findings indicated that ranolazine shortened APD_{80} and Ca_iTD_{80} in db/db mouse hearts, reduced the differences of APD_{80} and Ca_iTD_{80} between non-IR and IR zones, and attenuated the APD_{80} and Ca_iTD_{80} heterogeneity in both db/db and db/+ mouse hearts. Figure 2B shows representative examples of APD_{80} and Ca_iTD_{80} maps of the four groups. The db/db C mouse heart had the longest APD_{80} and Ca_iTD_{80}, which were longer in the IR zone than in the non-IR zone.

Table 1

Electrophysiological effects of ranolazine in isolated Langendorff-perfused mouse hearts after IR injury.

		APD_{80} (ms)		Ca_iTD_{80} (ms)		CV (cm/s)							
		200 ms	100 ms	200 ms	100 ms	200 ms	150 ms	120 ms	100 ms	90 ms	80 ms	70 ms	60 ms
db/db C (N = 11)	Non-IR	82 ± 9*	52 ± 7*	91 ± 7*	69 ± 5*	78 ± 13*	76 ± 13*	74 ± 14*	70 ± 13*	64 ± 12*	57 ± 13*	51 ± 12*	45 ± 12*
	IR	86 ± 9*	56 ± 6*	100 ± 9*	77 ± 8*	68 ± 18*	61 ± 16*	57 ± 15*	54 ± 14*	50 ± 12*	47 ± 11*	41 ± 10*	37 ± 10*
db/db R (N = 10)	Non-IR	70 ± 7	48 ± 6	84 ± 11	65 ± 6	88 ± 5	84 ± 8	80 ± 9	75 ± 8	74 ± 11	72 ± 12	64 ± 12	62 ± 10
	IR	73 ± 10	51 ± 6	89 ± 9	67 ± 5	82 ± 9	78 ± 8	76 ± 7	70 ± 6	67 ± 7	61 ± 6	58 ± 5	53 ± 6
db/+ C (N = 11)	Non-IR	75 ± 4	46 ± 4*	89 ± 7*	68 ± 3*	83 ± 15	78 ± 13*	75 ± 10*	70 ± 12*	67 ± 13*	60 ± 12*	57 ± 13*	52 ± 11*
	IR	78 ± 4	54 ± 4*	96 ± 10*	73 ± 6*	69 ± 12	64 ± 13*	59 ± 11*	55 ± 9*	51 ± 9*	46 ± 8*	43 ± 7*	38 ± 7*
db/+ R (N = 10)	Non-IR	71 ± 10	46 ± 2	84 ± 6	65 ± 4	90 ± 25	89 ± 25	85 ± 27	83 ± 28	80 ± 25	75 ± 23	67 ± 19	61 ± 17
	IR	73 ± 14	49 ± 5	86 ± 10	66 ± 5	86 ± 22	82 ± 21	80 ± 22	75 ± 24	72 ± 21	68 ± 22	64 ± 21	56 ± 16

Values are mean ± SD. APD_{80}, action potential duration at 80% repolarization; Ca_iTD_{80}, effective refractory period; CV, conduction velocity; IR, ischemia-reperfusion. * indicates P < 0.05 for non-IR vs. IR.

Ranolazine effects on Ca_i decay

Figure 3A shows the summarized results of Ca_i decay tau value among the four groups. Ca_i decay time was the longest in the db/db C group (P = 0.013). Ranolazine shortened the tau value more significantly in db/db mouse hearts (from 35.8 ± 3.8 ms to 31.5 ± 3.4 ms; P = 0.001) than in db/+ mouse hearts (from 32.8 ± 3.5 ms to 30.8 ± 3.9 ms; P = 0.083). Furthermore, Ca_i decay time was longer in the IR zone than in the non-IR zone. Ranolazine ameliorated the differences in the tau values between the non-IR and IR zones. As shown in Fig. 3A, the P values were increased from 0.044 to 0.055 (db/db C vs. db/db R) and from 0.066 to 0.118 (db/+ C vs. db/+ R). A representative example of Ca_i decay at the non-IR and IR zones in the four groups is shown in Fig. 3B.

Ranolazine effects on CV

Table 1 and Fig. 4A summarize the effects of 1-week ranolazine pretreatment on CV in mouse hearts with acute regional IR injury. Among the four groups, CV_{non-IR} did not differ significantly at all PCLs. However, CV_{IR} was significantly different at PCLs of 150, 120, 100, 90, 80, 70, and 60 ms (P = 0.022, 0.007, 0.013, 0.003, 0.004, 0.002, and 0.002, respectively). Post hoc analysis showed that the difference in CV_{IR} was mainly due to the pretreatment of ranolazine. Ranolazine ameliorated CV_{IR} slowing to improve conduction inhomogeneity. As shown in Fig. 4A, the difference between CV_{IR} and CV_{non-IR} was significant in the db/db C and db/+ C groups, but insignificant in the db/db R and db/+ R groups. Figure 4B shows an example of isochrone maps in the four groups. At PCL = 60 ms, the CV_{IR} was slower in the db/db C (44 cm/s) and db/+ C (46 cm/s) mice than in the db/db R (58 cm/s) and db/+ R (70 cm/s) mice, and the difference between CV_{IR} and CV_{non-IR} was also greater in the db/db C (17 cm/s) and db/+ C (17 cm/s) mice than in the db/db R (13 cm/s) and db/+ R (5 cm/s) mice.

Induction of spatially concordant and discordant alternans

Although spatially concordant alternans (SCA) could be provoked in all hearts in the four groups, the longest PCL required to provoke SCA was significantly shorter in the ranolazine groups (107 ± 15, 86 ± 5 ms in the db/db C, db/db R groups, respectively; 102 ± 15, 79 ± 17 ms in the db/+ C, db/+ R groups, respectively; P < 0.001). Similarly, spatially discordant alternans (SDA) could be provoked in all hearts, and the longest PCL required to provoke SDA was significantly shorter in the ranolazine groups (90 ± 12, 69 ± 11 ms in the db/db C, db/db R groups, respectively; 80 ± 14, 67 ± 9 ms in the db/+ C, db/+ R groups, respectively; P < 0.001). A representative example was shown in supplementary Fig. 1.

VA inducibility

VA inducibility was significantly different among the four groups: VA was induced in 10 of 11 (db/db C), 3 of 10 (db/db R), 7 of 11 (db/+ C) and 2 of 10 (db/+ R) hearts (P = 0.004). Figure 5 illustrates VT induction in a db/db C mouse heart. Figures 5A and 5B show images of IR creation and the mapping field, respectively. Figure 5C shows the V_m recordings at sites “a” (rotor anchoring site on a nodal line, Fig. 5E) and “b” (left ventricular base) during VT induction. Extrastimulus pacing led to dispersion of refractoriness and unidirectional conduction block (frame 310; Fig. 5D), and reentrant wavefronts were initiated after pacing (frames 346–509). During the initiation of VT, the core of reentrant wavefronts anchored at site “a,” where fragmented V_m transient is shown (Fig. 5C). Post hoc analysis revealed that ranolazine effectively suppressed the VA inducibility in both db/db and db/+ mouse hearts with acute regional IR injury (Fig. 5F)

Protein Expression

To elucidate the roles of Ca^{2+}-handling proteins, Na^+ channel, and Cx43 in the antiarrhythmic mechanisms of ranolazine, we measured and compared the levels of the associated proteins between the IR and non-IR zones. The results are presented in Fig. 6 and supplementary Fig. 2. In db/db C hearts, the expression levels of $pThr^{17}$-phospholamban, calsequestrin 2, and SCN5A in the IR zone were significantly lower than those in the non-IR zone. Ranolazine pretreatment attenuated the downregulation of these proteins in the IR zone by acute IR injury. In db/+ C hearts, the expression level of $pThr^{17}$-phospholamban was significantly lower than that in the non-IR zone, which was attenuated by ranolazine.

Ranolazine effects on $I_{Na,L}$ in cardiomyocytes from db/db and db/+ mice with acute IR injury

The db/db cardiomyocytes expressed a greater $I_{Na,L}$ density (0.420 ± 0.214 pA/pF, n = 93) than the db/+ cells (0.209 ± 0.056 pA/pF, n = 51, P < 0.001). As shown in Fig. 7A, ranolazine therapy significantly decreased the density of $I_{Na,L}$ in both db/db mice (0.497 ± 0.219 pA/pF, n = 61 in db/db C vs. 0.272 ± 0.096 pA/pF, n = 32 in db/db R, P = 0.034) and db/+ mice (0.229 ± 0.044 pA/pF, n = 15 in db/+ C vs. 0.201 ± 0.059 pA/pF, n = 36 in db/+ R, P = 0.047), but the density of $I_{Na,L}$ in db/db R group was still higher than those in db/+ C (P = 0.048) and db/+ R (P = 0.037) groups. There was significant difference of $I_{Na,L}$ density between IR and non-IR cardiomyocytes in the db/db C group (0.655 ± 0.168 pA/pF, n = 23 vs 0.402 ± 0.189 pA/pF, n = 38, P < 0.001), but not in the db/db R group (0.291 ± 0.076 pA/pF, n = 20 vs 0.240 ± 0.120 pA/pF, n = 12, P = 0.077).

Discussion

In this study, we found that 1-week ranolazine pretreatment significantly improved IR injury-induced conduction inhomogeneity and impaired Ca_i decay, reduced APD_{80} and Ca_iTD_{80} prolongation and heterogeneity, and suppressed the inducibility of arrhythmogenic alternans and VA. The in vivo electrophysiological studies show that the db/db C group was significantly more vulnerable to longer VT compared with the other three groups, suggesting that ranolazine pretreatment is effective in protecting db/db mice from IR-induced life-threatening VA. Patch clamp studies showed that db/db cardiomyocytes expressed a greater $I_{Na,L}$ density, which was significantly higher in the IR zone than the non-IR zone. Ranolazine significantly decreased the density of $I_{Na,L}$ and reduced the difference of $I_{Na,L}$ density between the IR and IR zones in diabetic mouse hearts. Western blotting showed that protein expression of $pThr^{17}$-phospholamban, calsequestrin 2, and SCN5A was significantly decreased in

the IR zone in diabetic mouse hearts, and ranolazine ameliorated the downregulation of these proteins, which at least partly underlie the molecular mechanisms of the antiarrhythmic actions of ranolazine in diabetic mouse hearts with regional IR injury.

Ranolazine Administration Improves Ca Dynamics In The Ir Zone

During IR injury, Ca_i overload can result from the impaired ability of sarcoendoplasmic reticular Ca^{2+}-ATPase (SERCA2a) to sequester cytosolic Ca^{2+} in stunned myocardium,[18] and from the enhanced $I_{Na,L}$ to increase Na^+ influx, and via reverse-mode NCX, to increase Ca_i.[9] $I_{Na,L}$ enhancement may also result in calcium/calmodulin protein kinase II activation, which may induce proarrhythmic sarcoplasmic reticulum (SR) Ca^{2+} leak.[19] It has been reported that mitochondrial Ca^{2+} uptake, binding of the L-type Ca^{2+} channel to the sarcolemma, and Ca^{2+} intake by SR are decreased in diabetic hearts.[20] In conjunction with an intrinsic higher $I_{Na,L}$, cellular dysregulation of Ca^{2+} homeostasis would be more pronounced in post-IR myocardial dysfunction and arrhythmogenicity in db/db mouse hearts.

Blockade of $I_{Na,L}$ may reverse the impaired Ca^{2+} cycling in conditions of increased $I_{Na,L}$. It has been shown that enhancement of $I_{Na,L}$ increases the vulnerability to Ca_i alternans during rapid pacing.[21] Fukaya et al. reported that ranolazine reduces diastolic Ca_i and mitigates cardiac alternans, representing a mechanism underlying the antiarrhythmic benefit of $I_{Na,L}$ blockade in heart failure.[22] Consistent with this, our data showed that ranolazine suppressed the induction of SCA and SDA in mouse hearts with IR injury. In addition to $I_{Na,L}$ blockade to ameliorate Ca_i overload, the presented data reveal some possible molecular mechanisms underlying the antiarrhythmic effects of ranolazine in the IR zone of diabetic hearts. Phospholamban is a key phosphorylation-dependent modulator of SERCA2a activity, and phospholamban dephosphorylation has been reported to account for myocardial stunning.[23] Our data show that ranolazine attenuated the downregulation of $pThr^{17}$-phospholamban in the IR zone, which played a role in accelerating Ca_i decay and shortening Ca_iTD_{80}. The Ca_i alternans suppression and Ca_iTD_{80} shortening were reported to reduce the susceptibility to subsequent refibrillation in a long-standing VF rabbit model.[24] Additionally, calsequestrin 2 is the main Ca^{2+}-binding protein of the SR, serving as an important regulator of Ca^{2+} to protect the heart against premature Ca^{2+} release and triggered arrhythmias.[25] Downregulation of calsequestrin 2 increases SR Ca^{2+} leak and arrhythmia susceptibility under stress.[26] Our data show decreased expression of calsequestrin 2 in the IR zone of diabetic hearts, which may partly account for the increased VA inducibility in the db/db C group. Parikh et al. reported that ranolazine stabilizes cardiac ryanodine receptors to inhibit Ca_i oscillations and early afterdepolarizations.[27] The amelioration of calsequestrin 2 downregulation in the IR zone by ranolazine may have contributed to the reduced VA inducibility in the db/db R group in the present study.

It was reported that cardiac IR injury is accompanied by a marked reduction in SR Ca^{2+}-pump ATPase, Ca^{2+}-uptake and Ca^{2+}-release activities, and the mRNA levels for SR Ca^{2+}-handling proteins such as SERCA2a, ryanodine receptor, calsequestrin and phospholamban were decreased in the ischemia-reperfused heart as compared with the non-ischemic control.[28] Our data also shows that protein expression of pThr17-phospholamban, calsequestrin 2, and SCN5A was significantly decreased in the IR zone in diabetic mouse hearts, and ranolazine ameliorated the downregulation of these proteins. We do not know the exact mechanisms. Upon reperfusion of ischemic myocardium, the sudden availability of oxygen in the ischemic myocardium increases the formation of reactive oxygen species and intracellular Ca^{2+} overload, which cause cell damage and apoptosis. Because ranolazine was reported to reduce oxidative stress and Ca^{2+} overload, and to improve mitochondrial integrity during IR,[10] these actions may underlie the mechanism of ameliorating IR injury, including the downregulation of pThr17-phospholamban, calsequestrin 2, and SCN5A by ranolazine pretreatment.

Ranolazine Administration Ameliorates Conduction Inhomogeneity In Regional Ir Injury

Studies have shown reduced cardiac conduction reserve in diabetic animal models.[12, 29, 30] Therefore, propagation of activity through the myocardium in diabetic hearts is more sensitive to conditions influencing cellular excitability or intercellular electrical coupling. For example, more pronounced activation of Ca^{2+}-independent phospholipase A_2 in response to acute ischemia was reported to contribute to arrhythmogenic conduction slowing in the diabetic rat heart.[31] In the regional IR model, the elevated Ca_i in the IR myocardium may prolong refractoriness by stimulating NCX current and thereby prolong APD,[32] which interferes with wavefront propagation. The effect of ranolazine on APD depends on the relative contributions of $I_{Na,L}$ and rapidly activating delayed rectifier potassium current to repolarization.[9] Ranolazine abbreviates APD and thereby refractoriness in conditions when $I_{Na,L}$ is enhanced. Our data show that ranolazine shortened APD_{80}, especially in the IR zone, which may conjoin with the attenuated downregulation of SCN5A in the IR zone to improve CV_{IR} in db/db mouse hearts. In addition, ranolazine, by shifting myocardial utilization of fatty acid to glucose during reperfusion, reduces deleterious lipid metabolites.[33] These lipid metabolites have been shown to cause uncoupling of gap junctions.[34] It is possible that ranolazine improves CV_{IR} via its beneficial effects on myocardial metabolism.

Conclusions

Ranolazine pretreatment shortens APD_{80} and Ca_iTD_{80}, reduces Ca_i decay time, and ameliorates conduction velocity inhomogeneity to suppress induction of arrhythmogenic alternans and VA; and amelioration of downregulation of $pThr^{17}$-phospholamban, calsequestrin 2 and SCN5A may partly underlie the anti-arrhythmic molecular mechanisms of ranolazine in db/db mouse hearts with IR injury.

Abbreviations

APD_{80}
Action potential duration at 80% repolarization
Ca_i
intracellular Ca^{2+}
Ca_iTD_{80}
Ca_i transient duration at 80% decay
CV
conduction velocity
CV_{IR}
conduction velocity measured from the pacing site to the left ventricular apex
CV_{non-IR}
conduction velocity along an axis parallel to the atrioventricular ring
$I_{Na,L}$
late sodium current
IR
ischemia-reperfusion
NCX
Na^+/Ca^{2+} exchanger
PCL
pacing cycle length
SCA
spatially concordant alternans
SDA
spatially discordant alternans
SERCA2a
sarcoendoplasmic reticular Ca^{2+}-ATPase
SR
sarcoplasmic reticulum
VA
ventricular tachyarrhythmia
VF
ventricular fibrillation
V_m
membrane voltage
VT
ventricular tachycardia

Declarations

Ethical approval and consent to participate: This study protocol was approved by the Institutional Animal Care and Use Committee of Chang Gung Memorial Hospital (approval no. 2015092401) and conformed to the current NIH guidelines for the care and use of laboratory animals.

Consent for publication: not applicable

Availability of data and materials: The datasets used during the current study are available from the corresponding author on reasonable request.

Competing interests: All authors have no conflict of interest.

Funding: This study was funded by Chang Gung Medical Research Program (grant number: CMRPG3F035).

Authors' contributions: CC performed optical mapping experiments, interpreted mapping data and was a major contributor in writing the manuscript. HL assisted in animal model creation and helped analyzed mapping data. GJ helped performing patch-clamp experiments. HT, TH and HT were engaged in Western blot experiments. MS and Y supervised Western blot experiments and interpreted data. PC helped performing all parts of experiments and revised the manuscript. All authors read and approved the final manuscript."

Acknowledgments: This study was supported by a grant from Chang Gung Medical Research Program, Taiwan, CMRPG3F035 to C.C. Chou.

References

1. Jones SP, Girod WG, Granger DN, Palazzo AJ, Lefer DJ: **Reperfusion injury is not affected by blockade of P-selectin in the diabetic mouse heart**. *American Journal of Physiology-Heart and Circulatory Physiology* 1999, **277**(2):H763-H769.
2. Lefer DJ, Scalia R, Jones SP, Sharp BR, Hoffmeyer MR, Farvid AR, Gibson MF, Lefer AM: **HMG-CoA reductase inhibition protects the diabetic myocardium from ischemia-reperfusion injury**. *The FASEB Journal* 2001, **15**(8):1454-1456.
3. Anzawa R, Bernard M, Tamareille S, Baetz D, Confort-Gouny S, Gascard JP, Cozzone P, Feuvray D: **Intracellular sodium increase and susceptibility to ischaemia in hearts from type 2 diabetic db/db mice**. *Diabetologia* 2006, **49**(3):598-606.
4. Greer JJ, Ware DP, Lefer DJ: **Myocardial infarction and heart failure in the db/db diabetic mouse**. *Am J Physiol Heart Circ Physiol* 2006, **290**(1):H146-153.
5. Tani M, Neely JR: **Role of intracellular Na+ in Ca2+ overload and depressed recovery of ventricular function of reperfused ischemic rat hearts. Possible involvement of H+-Na+ and Na+-Ca2+ exchange**. *Circulation research* 1989, **65**(4):1045-1056.
6. Ward CA, Giles WR: **Ionic mechanism of the effects of hydrogen peroxide in rat ventricular myocytes**. *The Journal of Physiology* 1997, **500**(3):631-642.
7. MA Jh, LUO At, ZHANG Ph: **Effect of hydrogen peroxide on persistent sodium current in guinea pig ventricular myocytes**. *Acta Pharmacologica Sinica* 2005, **26**(7):828-834.
8. Lu Z, Jiang Y-P, Wu C-YC, Ballou LM, Liu S, Carpenter ES, Rosen MR, Cohen IS, Lin RZ: **Increased persistent sodium current due to decreased PI3K signaling contributes to QT prolongation in the diabetic heart**. *Diabetes* 2013, **62**(12):4257-4265.
9. Antzelevitch C, Burashnikov A, Sicouri S, Belardinelli L: **Electrophysiologic basis for the antiarrhythmic actions of ranolazine**. *Heart Rhythm* 2011, **8**(8):1281-1290.
10. Aldakkak M, Camara AK, Heisner JS, Yang M, Stowe DF: **Ranolazine reduces Ca2+ overload and oxidative stress and improves mitochondrial integrity to protect against ischemia reperfusion injury in isolated hearts**. *Pharmacological research* 2011, **64**(4):381-392.
11. Dhalla AK, Wang W-Q, Dow J, Shryock JC, Belardinelli L, Bhandari A, Kloner RA: **Ranolazine, an antianginal agent, markedly reduces ventricular arrhythmias induced by ischemia and ischemia-reperfusion**. *American Journal of Physiology-Heart and Circulatory Physiology* 2009, **297**(5):H1923-H1929.
12. Chou CC, Ho CT, Lee HL, Chu Y, Yen TH, Wen MS, Lin SF, Lee CH, Chang PC: **Roles of impaired intracellular calcium cycling in arrhythmogenicity of diabetic mouse model**. *Pacing and Clinical Electrophysiology* 2017, **40**(10):1087-1095.
13. Rajab M, Jin H, Welzig CM, Albano A, Aronovitz M, Zhang Y, Park H-J, Link MS, Noujaim SF, Galper JB: **Increased inducibility of ventricular tachycardia and decreased heart rate variability in a mouse model for type 1 diabetes: effect of pravastatin**. *American Journal of Physiology-Heart and Circulatory Physiology* 2013, **305**(12):H1807-H1816.
14. Chang PC, Huang YC, Lee HL, Chang GJ, Chu Y, Wen MS, Chou CC: **Inhomogeneous Down-regulation of INa underlies piceatannol pro-arrhythmic Mechanism in regional ischemia-reperfusion**. *Pacing and Clinical Electrophysiology* 2018, **41**(9):1116-1122.
15. Chou CC, Chang PC, Wei YC, Lee KY: **Optical mapping approaches on muscleblind-like compound knockout mice for understanding mechanistic insights into ventricular arrhythmias in myotonic dystrophy**. *Journal of the American Heart Association* 2017, **6**(4):e005191.
16. Chang G-J, Chang C-J, Chen W-J, Yeh Y-H, Lee H-Y: **Electrophysiological and mechanical effects of caffeic acid phenethyl ester, a novel cardioprotective agent with antiarrhythmic activity, in guinea-pig heart**. *European journal of pharmacology* 2013, **702**(1-3):194-207.
17. Chou C-C, Chang P-C, Wen M-S, Lee H-L, Wo H-T, Yeh S-J, Wu D: **Piceatannol facilitates conduction block and ventricular fibrillation induction in ischemia-reperfused rabbit hearts with pacing-induced heart failure**. *International journal of cardiology* 2014, **171**(2):250-258.
18. Limbruno U, Zucchi R, Ronca-Testoni S, Galbani P, Ronca G, Mariani M: **Sarcoplasmic reticulum function in the "stunned" myocardium**. *Journal of molecular and cellular cardiology* 1989, **21**(10):1063-1072.
19. Sag CM, Mallwitz A, Wagner S, Hartmann N, Schotola H, Fischer TH, Ungeheuer N, Herting J, Shah AM, Maier LS: **Enhanced late INa induces proarrhythmogenic SR Ca leak in a CaMKII-dependent manner**. *Journal of molecular and cellular cardiology* 2014, **76**:94-105.

20. Pereira L, Ruiz-Hurtado G, Rueda A, Mercadier J-J, Benitah J-P, Gómez AM: **Calcium signaling in diabetic cardiomyocytes**. *Cell calcium* 2014, **56**(5):372-380.
21. Wasserstrom JA, Sharma R, O'Toole MJ, Zheng J, Kelly JE, Shryock J, Belardinelli L, Aistrup GL: **Ranolazine antagonizes the effects of increased late sodium current on intracellular calcium cycling in rat isolated intact heart**. *Journal of Pharmacology and Experimental Therapeutics* 2009, **331**(2):382-391.
22. Fukaya H, Plummer BN, Piktel JS, Wan X, Rosenbaum DS, Laurita KR, Wilson LD: **Arrhythmogenic cardiac alternans in heart failure is suppressed by late sodium current blockade by ranolazine**. *Heart rhythm* 2019, **16**(2):281-289.
23. Kim S-J, Kudej RK, Yatani A, Kim Y-K, Takagi G, Honda R, Colantonio DA, Van Eyk JE, Vatner DE, Rasmusson RL: **A novel mechanism for myocardial stunning involving impaired Ca2+ handling**. *Circulation research* 2001, **89**(9):831-837.
24. Azam MA, Zamiri N, Massé S, Kusha M, Lai PF, Nair GK, Tan NS, Labos C, Nanthakumar K: **Effects of late sodium current blockade on ventricular refibrillation in a rabbit model**. *Circulation: Arrhythmia and Electrophysiology* 2017, **10**(3):e004331.
25. Novák P, Soukup T: **Calsequestrin distribution, structure and function, its role in normal and pathological situations and the effect of thyroid hormones**. *Physiological research* 2011, **60**(3):439.
26. Chopra N, Kannankeril PJ, Yang T, Hlaing T, Holinstat I, Ettensohn K, Pfeifer K, Akin B, Jones LR, Franzini-Armstrong C: **Modest reductions of cardiac calsequestrin increase sarcoplasmic reticulum Ca2+ leak independent of luminal Ca2+ and trigger ventricular arrhythmias in mice**. *Circulation research* 2007, **101**(6):617-626.
27. Parikh A, Mantravadi R, Kozhevnikov D, Roche MA, Ye Y, Owen LJ, Puglisi JL, Abramson JJ, Salama G: **Ranolazine stabilizes cardiac ryanodine receptors: a novel mechanism for the suppression of early afterdepolarization and torsades de pointes in long QT type 2**. *Heart Rhythm* 2012, **9**(6):953-960.
28. Takeo S, Nasa Y, Tanonaka K, Yamaguchi F, Yabe K-i, Hayashi H, Dhalla NS: **Role of cardiac renin-angiotensin system in sarcoplasmic reticulum function and gene expression in the ischemic-reperfused heart**. *Molecular and cellular biochemistry* 2000, **212**(1-2):227-235.
29. Nygren A, Olson M, Chen K, Emmett T, Kargacin G, Shimoni Y: **Propagation of the cardiac impulse in the diabetic rat heart: reduced conduction reserve**. *The Journal of physiology* 2007, **580**(2):543-560.
30. Olsen KB, Axelsen LN, Braunstein TH, Sorensen CM, Andersen CB, Ploug T, Holstein-Rathlou NH, Nielsen MS: **Myocardial impulse propagation is impaired in right ventricular tissue of Zucker diabetic fatty (ZDF) rats**. *Cardiovasc Diabetol* 2013, **12**:19.
31. Rahnema P, Shimoni Y, Nygren A: **Reduced conduction reserve in the diabetic rat heart: role of iPLA2 activation in the response to ischemia**. *American Journal of Physiology-Heart and Circulatory Physiology* 2010, **300**(1):H326-H334.
32. Shiferaw Y, Watanabe M, Garfinkel A, Weiss J, Karma A: **Model of intracellular calcium cycling in ventricular myocytes**. *Biophysical journal* 2003, **85**(6):3666-3686.
33. McCormack JG, Barr RL, Wolff AA, Lopaschuk GD: **Ranolazine stimulates glucose oxidation in normoxic, ischemic, and reperfused ischemic rat hearts**. *Circulation* 1996, **93**(1):135-142.
34. Arnsdorf MF, Sawicki GJ: **The effects of lysophosphatidylcholine, a toxic metabolite of ischemia, on the components of cardiac excitability in sheep Purkinje fibers**. *Circulation research* 1981, **49**(1):16-30.

Figures

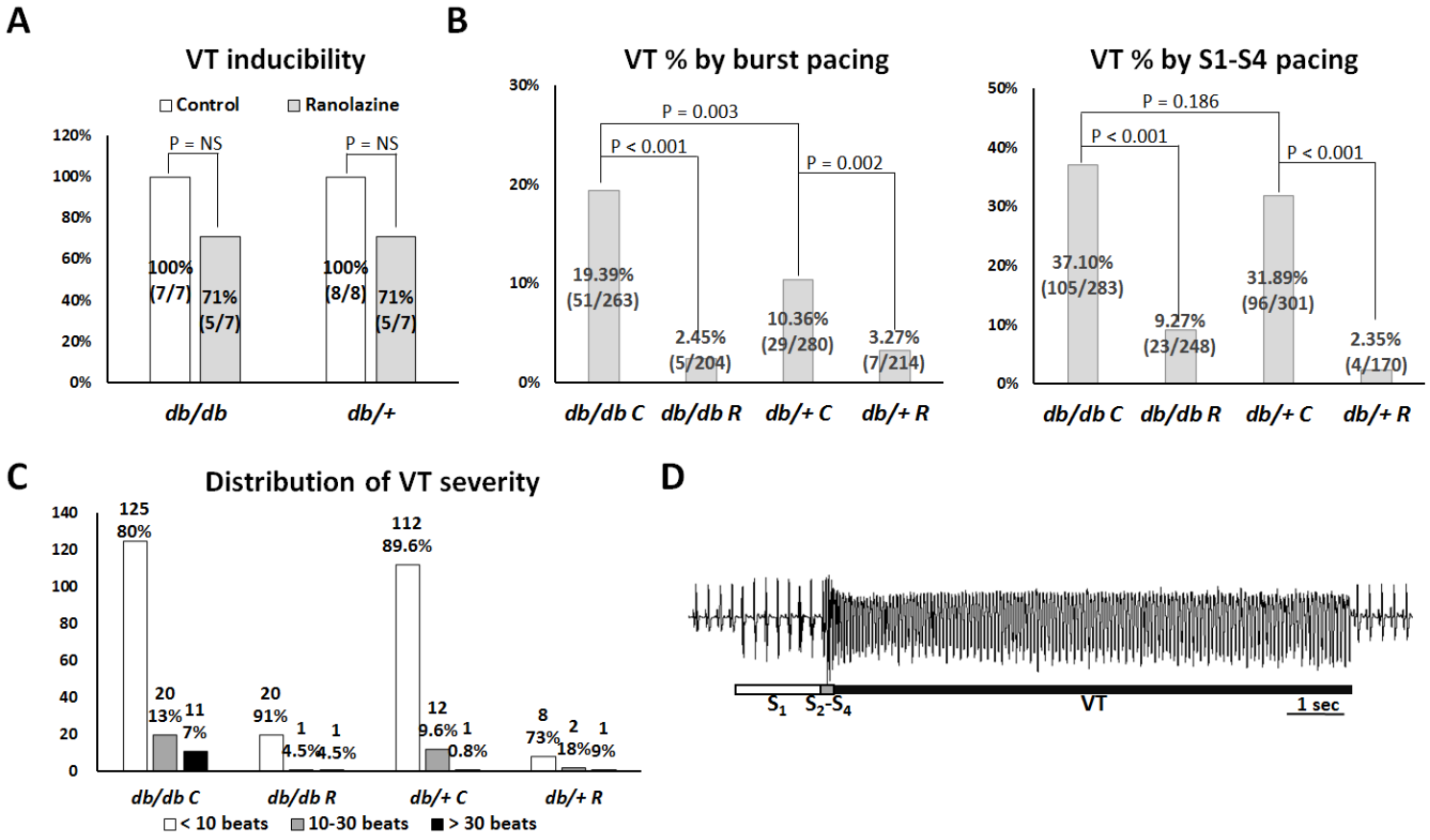

Figure 1

In vivo electrophysiological study. (A) Summary of in vivo ventricular tachycardia (VT) inducibility. (B) percentage of VT episodes by pacing protocols. The number and percentage of pacing-induced VT were shown in the middle of each bar. (C) Distribution of the severity of VT, plotted as the number of beats of VT. The number and percentage of VT episodes were shown on the top of each bar. (D) Representative example of pseudo-electrocardiogram showing extrastimulus pacing-induced VT in a db/db C mouse heart.

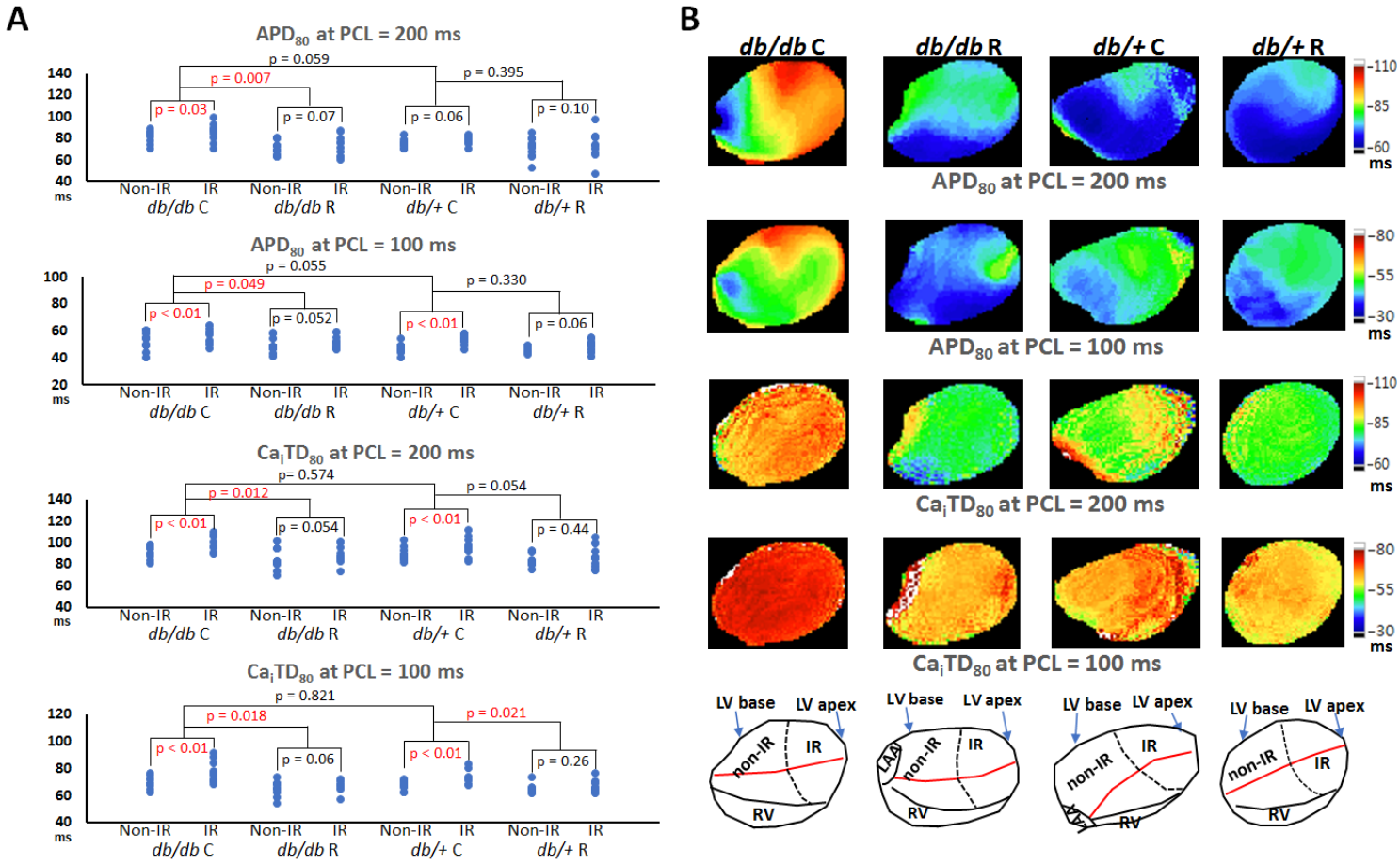

Figure 3

Effects of ranolazine on APD80 and CaiTD80. (A) Summarized results. (B) APD80 and CaiTD80 maps at pacing cycle length (PCL) = 200 and 100 ms.

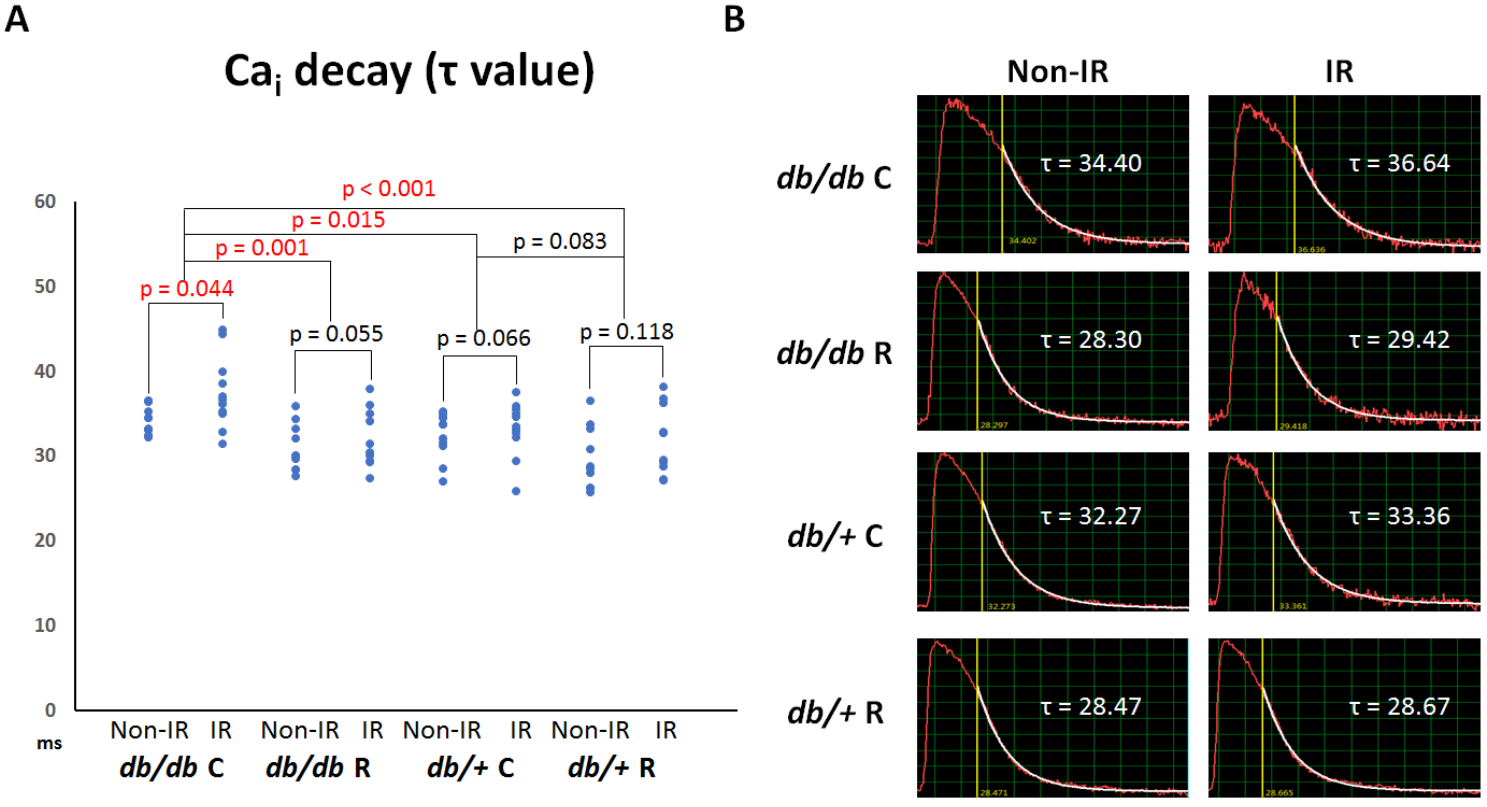

Figure 5

Effects of ranolazine on intracellular Ca2+ (Cai) decay. (A) Summary of Cai decay tau values among the four groups and between the ischemia–reperfusion (IR) and non-IR zones. (B) Representative examples of Cai decay in the non-IR and IR zones.

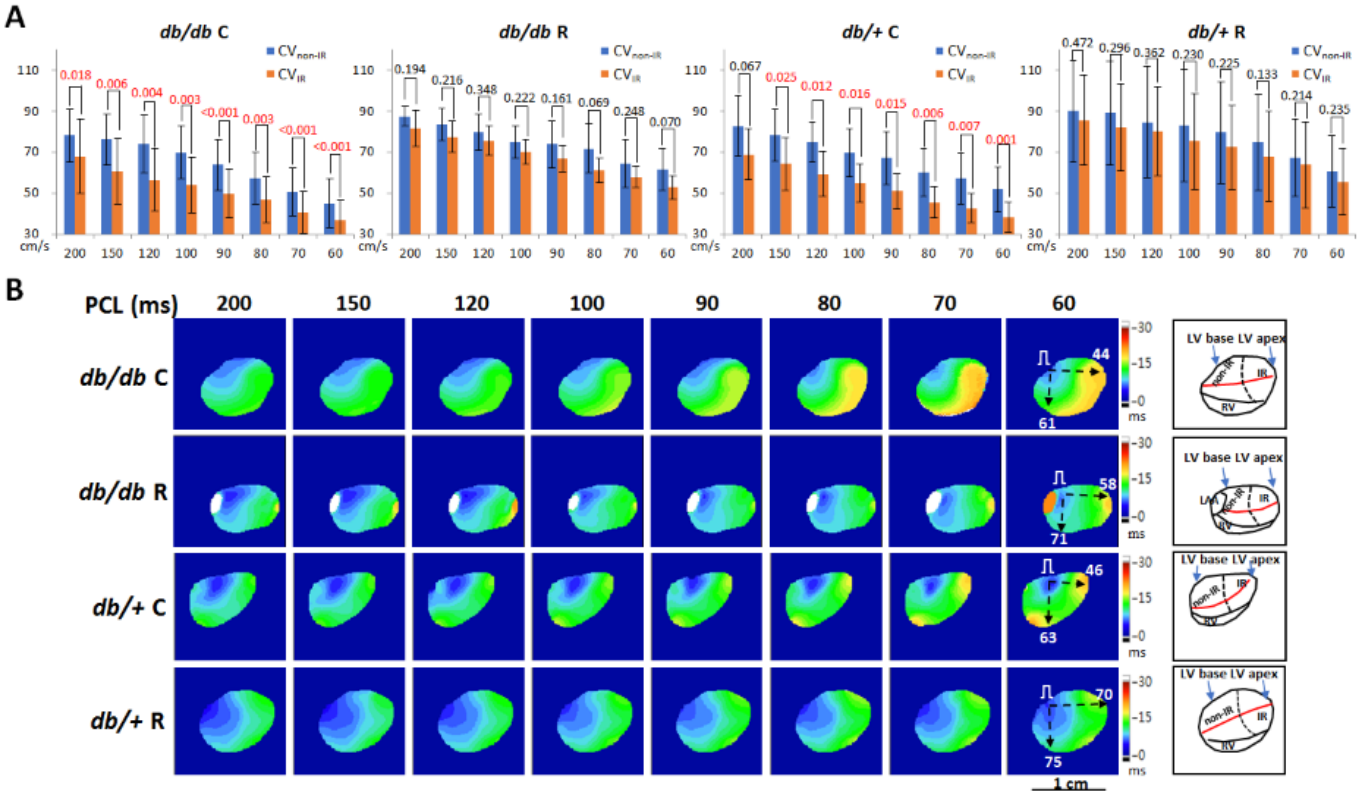

Figure 7

Effects of ranolazine on conduction velocity (CV). (A) Summary of CV measured from the pacing site along the atrioventricular ring (CVnon-IR) and to the left ventricular apex (CVIR). (B) Isochrone maps at a pacing cycle length (PCL) from 200 to 60 ms. Black dashed arrows indicate the directions of CVnon-IR and CVIR measurements; numbers in right subpanels are CV (cm/s). Right subpanels show the anatomical structure and orientation of optical maps. Red line, left coronary artery; dashed line, margin of IR zone; LAA, left atrial appendage; LV, left ventricle; RV, right ventricle.

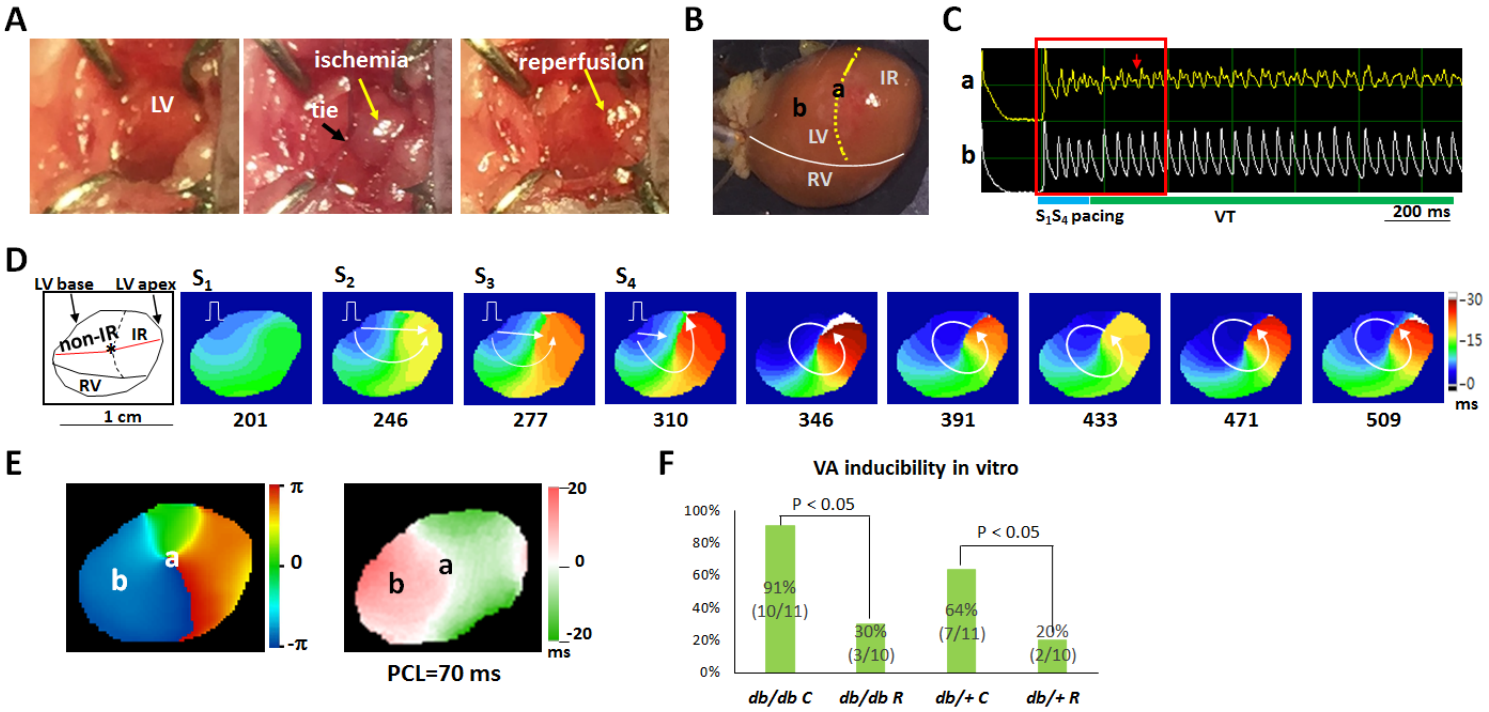

Figure 9

Ventricular tachycardia (VT) induction in a db/db C mouse heart with ischemia–reperfusion (IR) injury. (A) IR creation. Ischemia zone distal to the tie is shown in gray, and recovered after removal of the ligature in red. (B) Mapping field. Yellow dotted line indicates the margin of the IR zone. LV, left ventricle; RV, right ventricle. (C) Membrane voltage (Vm) traces showing the initiation of VT by S1-S4 pacing. Red arrow indicates fragmented Vm transient during rotor anchoring at site “a”. (D) Isochrone maps corresponding to the period marked by a red square in C. The number below each frame is the time (ms) with the onset of data acquisition as time zero. White arrows indicate the directions of wavefront propagation. Left subpanel shows the anatomical structure of the mapping filed. Red line, left coronary artery; dashed line, margin of IR zone. (E) Phase singularity (left) and Vm alternans (right) maps. A phase singularity (site “a”) was formed on a nodal line during VT. (F) Summary of the VA inducibility result.

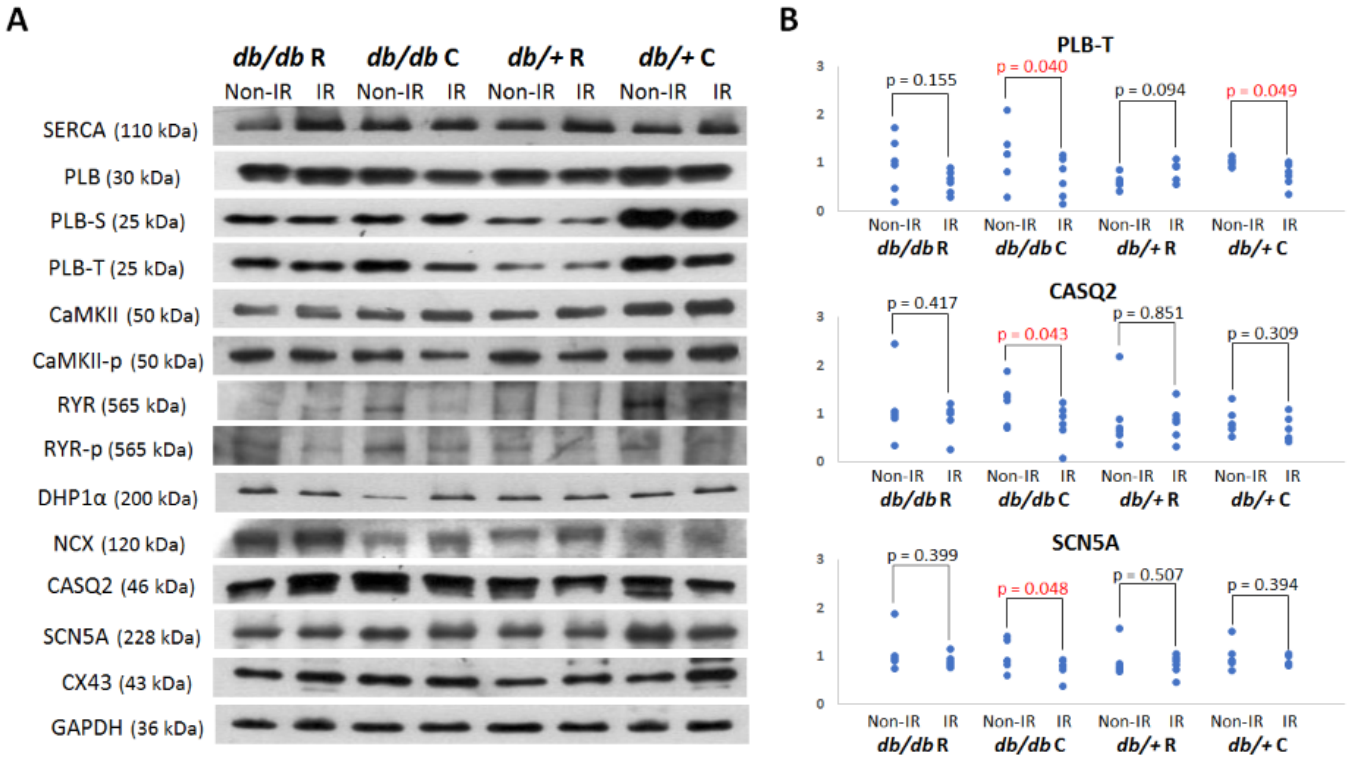

Figure 11

Western blotting results. Panels show representative bands (A) and scattered graphs represent densitometric values normalized to the corresponding GAPDH (B). RYR-p, pSer2808-RYR; CaMKII-p, pThr287-CaMKII.

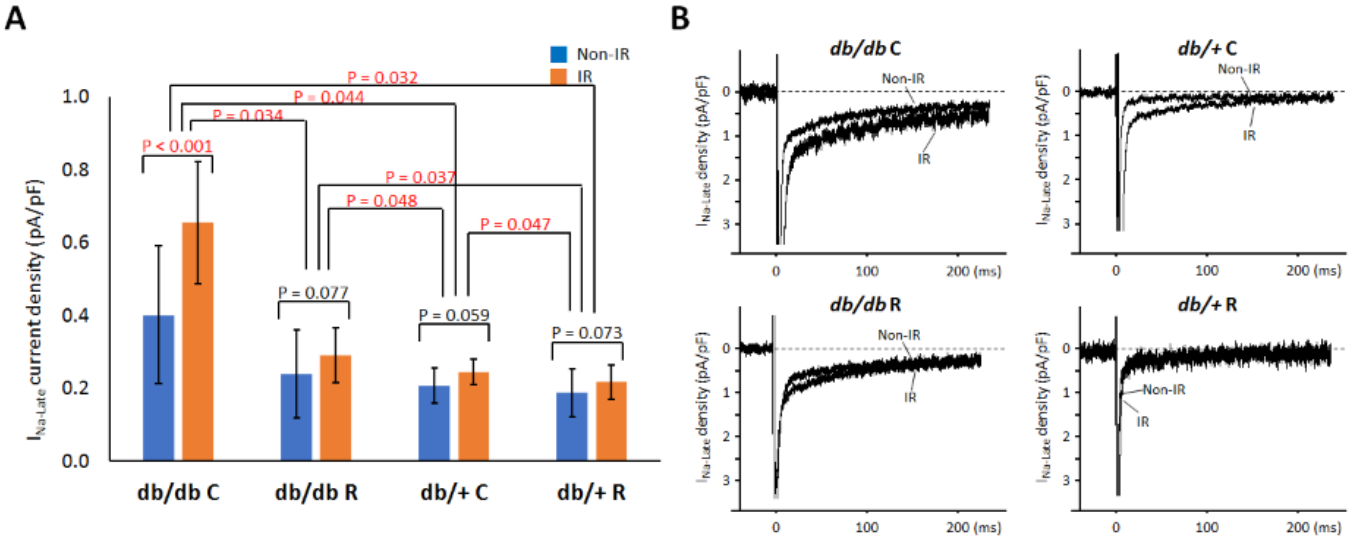

Figure 13

Whole-cell late Na+ currents (INa,L) recording. (A) Summarized data of mean INa,L. The graph shows the comparisons of the current density among four groups and between the ischemia–reperfusion (IR) and non-IR zones. (B) Representative INa,L traces of the cardiomyocytes among the four groups.

Supplementary Files

This is a list of supplementary files associated with this preprint. Click to download.

- Supplementalmaterial0311.pdf
- Supplementalmaterial0311.pdf